Helioseismology:
Study of the radial oscillation profile of the Sun: GOLF vs. MESA/GYRE

Afonso Sequeira Azenha (96502) - *Masters in Engineering Physics*

November 8, 2023

Abstract

The spectrum of the Sun's radial oscillations, corresponding to 183 days, from the GOLF (Global Oscillations at Low Frequencies) experiment, aboard SoHO (Solar and Heliospheric Observatory), is thoroughly analysed, from which we extract its *Fourier* spectrum. From said spectrum, we are able to obtain the solar eigenmode frequencies, which will be compared against simulation results from MESA/-GYRE. This simulation is run using the Asplund, 2009, solar model, instead of the Grevesse, 1998, since the former is more consistent with what is observed experimentally (Basu et *Al.*, 2009), as far as the Sun's sound speed profile is concerned. This entire analysis is also presented in this work. The comparison of these two models (MESA/GYRE and GOLF) is then explored, through the lights of: large and small separation plots, as well as their asymptotic limits; and *Echelle* diagrams. In general, we find a reasonably good agreement between simulation (MESA/GYRE) and experiment (GOLF), which validates our theoretical models, used to operate the simulations.

1 Introduction

Rather recently, the analysis of helioseismic data has opened the door to new and more refined techniques for probing the solar interior with unprecedented precision. At this point, one can be utterly sure that we do, in fact, know substantially more about the solar interior than we do about our own Earth's. Helioseismology is, for the most part, based on the analysis of the Sun's radial oscillation spectrum. Said spectrum, in turn, is obtained from the Doppler shift of the Na D line, in the Sun's radiation spectrum (Ref. [1]). This Doppler shift is then calibrated, using specially designed procedures, to generate a (radial) velocity time-series, that one can now analyse extensively to infer the Sun's characteristics. In this work, we will present the analysis of said time-series, obtained from the GOLF (Global Oscillations at Low Frequencies) experiment aboard the SoHO (Solar and Heliospheric Observatory) observatory. The results obtained from this analysis will be compared against theoretical simulations using the MESA (Modules for Experiments in Stellar Astrophysics) software, coupled with the GYRE package, used to determine the eigenfrequencies of the Sun's oscillations.

1.1 Theoretical considerations

The oscillations of the Sun's surface can be readily decomposed in terms of their eigenmodes, with frequencies $\nu_{n,l,m}$, where $l < n$ and $-l < m < l$. They are thoroughly characterised by these three quantum numbers, respectively: radial order, n, angular degree, l, and azimuthal order, m. Additionally, these eigenmodes can be of one of two types[1]: p-modes, when the restoring force is pressure, or g-modes, when the restoring force is gravity, more specifically, buoyancy. These two types of mode are fundamentally different, with g-modes being highly elusive to our detectors (Ref. [2]); p-modes, on the other hand, can be rather easily isolated and identified in the data that we have available today. For this work, these are the modes that we are interested in.

Mathematically, for these types of radial oscillations, one can generally write the pressure perturbation as:

$$p'(r,\theta,\phi,t) = \sqrt{4\pi}\,\mathrm{Re}\Big\{\tilde{p}'(r)Y_l^m(\theta,\phi)e^{-2\pi i\nu_{n,l,m}t}\Big\} \quad (1)$$

Here, we identify the usual spherical harmonic, $Y_l^m(\theta,\phi)$, and an amplitude function $\tilde{p}'(r)$, which depends only on r. Furthermore, in writing this, we assume a $2l+1$-fold degeneracy for every value of the azimuthal order m, i.e., $-l < m < l$. In practice, though, we will not be too concerned about this m value.

For low angular degrees ($n >> l$), we know, from Ref. [3] (Tassoul 1980), that the p-mode frequencies satisfy

$$\nu_{n,l} \approx (n + \frac{l}{2} + \frac{1}{4} + \alpha)\Delta\nu, \quad (2)$$

where α depends solely on the reflecting properties of the surface. Additionally,

$$\Delta\nu = \left(2\int_0^{R_\odot}\frac{dr}{c}\right)^{-1}, \quad (3)$$

---

[1]Actually, there's a third type: Surface gravity waves, but we won't be studying those here.

corresponds to the **large separation**, i.e., the inverse of the sound travel time through the diameter of the Sun. In practice, this is equivalent to the separation in frequency between adjacent modes of oscillation, having the same angular degree, l, but different radial order, n, i.e.,

$$\Delta\nu \approx \nu_{n,l} - \nu_{n-1,l} \tag{4}$$

The deviations from the simple relation (2) have considerable diagnostic potential. By extending our model to take into account the variation of c (sound speed) in the core, one finds (Gough, 1986; see also Tassoul, 1980, Ref. [3]):[2]

$$\delta\nu \equiv d_{n,l} = \nu_{n+1,l} - \nu_{n,l+2} \approx$$
$$\approx -(4l+6)\frac{\Delta\nu}{4\pi^2\nu_{nlm}}\int_0^{R_\odot} \frac{dr}{r}\frac{dc}{dr} \tag{5}$$

As can be seen, the integral is predominantly weighted towards the center of the star, as a result of the r^{-1} factor in the integrand. This behaviour is especially relevant as a diagnostic tool of the structure of stellar cores. More specifically, knowing that the core sound speed is reduced as μ (molecular weight) increases, with the conversion of hydrogen to helium as the star ages, we expect $d_{n,l}$ to decrease, thus providing a measure of the evolutionary state of the star in question. This $d_{n,l}$ quantity takes the name of **small separation**.

1.2 The MESA simulation package

In this work, we will make use of the "Modules for Experiments in Stellar Astrophysics" (MESA) software for creating various models of the Sun, with differing compositions and attributes. As the name suggests, MESA allows users to run experiments/simulations in stellar evolution, which constitutes a basic, yet paramount, tool that enables a broad range of research in astrophysics. Such MESA results are, afterwards, coupled to GYRE, which, in turn, allows for the determination of the Sun's radial oscillations' eigenmodes.

2 Part 1: Modelling the Sun

In the first part of our work, we will use MESA to simulate the evolution of the Sun, using two different solar models: Grevesse and Sauval (1998), Ref [5],

and Asplund et al. (2009), Ref. [6]. The end goal of this Part 1 is to figure out which of these models fares the best, in terms of better simulating our Sun. A comparison will be established based on the obtained solar sound speed profiles.

2.1 Model 1: Grevesse and Sauval (1998)

This first paper (Ref. [5]), written by Grevesse and Sauval, reviews the chemical composition of the Sun, essentially derived from the analysis of the solar photospheric spectrum. Among other things, they systematically determine the classical mass abundances:

1. X (Hydrogen mass fraction) = 0.735;

2. Y (Helium mass fraction) = 0.248;

3. Z (Heavy mass fraction) = 0.017.

Naturally, $X + Y + Z = 1$, as expected, and, in this case, we have $Z/X = 0.023$.

2.1.1 MESA parameters

At this point, we are ready to build the Grevesse solar model in MESA. Besides including the previously mentioned classical mass abundances, MESA requires that we specify the correct initial metal composition, `initial_zfracs = 3` (for gs98), and the relevant opacities, κ. For this, we use the following values (for the opacities), characteristic of this model, and already pre-built into MESA:

1. `kap_file_prefix = 'OP_gs98'`;

2. `kap_lowT_prefix = 'lowT_fa05_gs98'`.

Additionally, one also needs to specify the initial stellar mass, which in our case is simply $1M_\odot$. Finally, we tell MESA to stop its simulation as soon as the Sun's age reaches 4.603×10^9 y, i.e., the current solar age, since we are interested in comparing this simulation against other experimental results (GOLF, on SoHO).

2.1.2 Sound speed profile

The first result that we are interested in is the solar sound speed profile. The obtained plots are presented below.

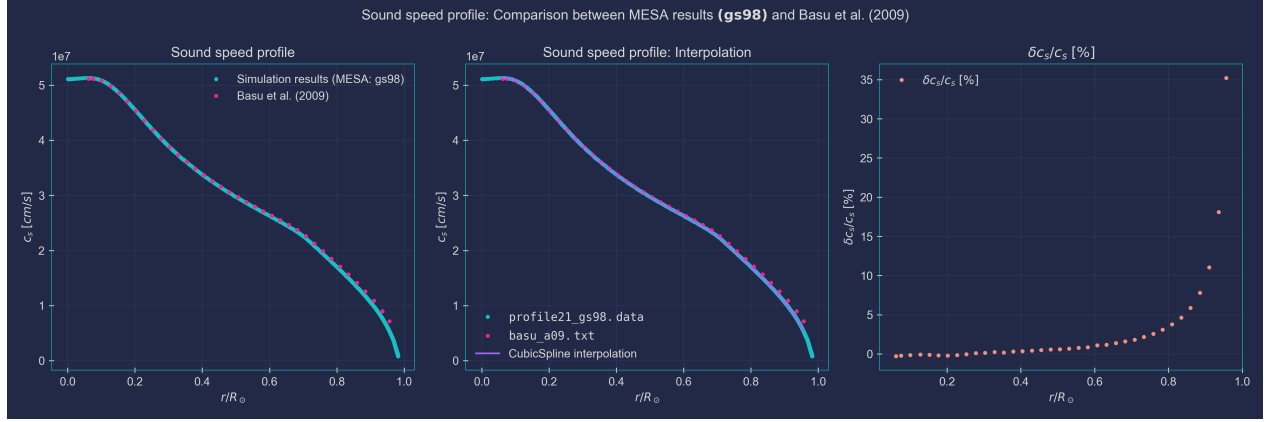[2]This expression was taken from Christensen-Dalsgaard's review on Helioseismology, Ref. [4].

Figure 1: Obtained sound speed profile for the Grevesse (1998) model. From left to right: Comparison with experimental data, based on inversion techniques, obtained by Basu et Al. (2009); Interpolation of the MESA results to the Basu points; Comparison between simulation and experiment.

Experimental data is also shown, from Basu et Al. (2009), Ref. [7], relative to which we compute the relative error (Third plot), as:

$$\delta c_s/c_s(\%) = \frac{c_{\text{Basu}} - c_{\text{MESA}}}{c_{\text{MESA}}} \times 100\% \qquad (6)$$

This will be used as a metric to compare the two models (gs98 and a09). Additionally, note that, in order to compare the simulation to Basu's experimental values, we had to interpolate MESA's results to Basu's $r/R_\odot$ values (See middle plot). This is done using the CubicSpline interpolation method, from scipy.

2.2 Model 2: Asplund et al. (2009)

This more recent model, from Ref. [6], considers:

1. X (Hydrogen mass fraction) = 0.7381;

2. Y (Helium mass fraction) = 0.2485;

3. Z (Heavy mass fraction) = 0.0134.

This way, $Z/X = 0.0182$.

2.2.1 MESA parameters

Additionally, it uses initial_zfracs = 6 (for a09), for the initial metal composition, and:

1. kap_file_prefix = 'OP_a09_nans_removed_by_hand';

2. kap_lowT_prefix = 'lowT_fa05_a09p',

for the opacities.

2.2.2 Sound speed profile

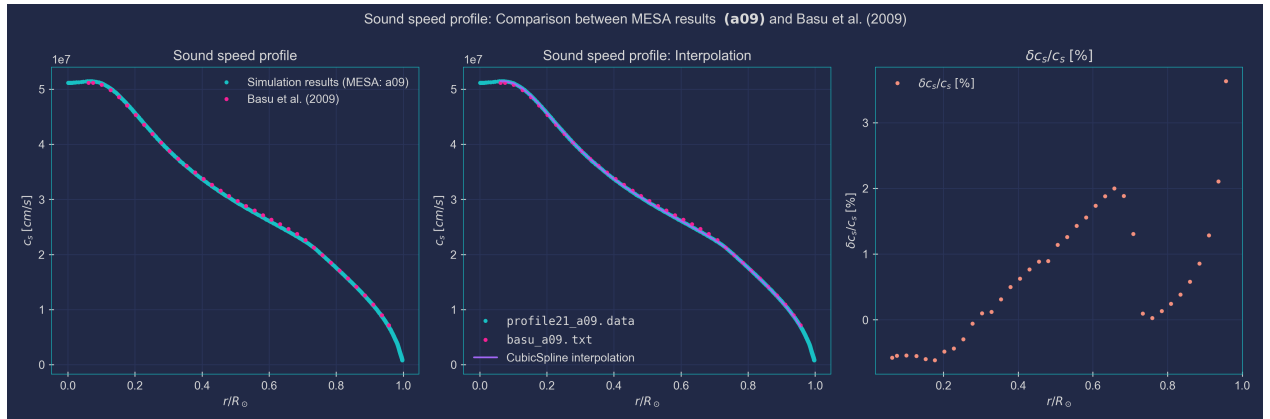For this model, the obtained sound speed profile is presented below.

Figure 2: Obtained sound speed profile for the Asplund (2009) model. From left to right: Comparison with experimental data, based on inversion techniques, obtained by Basu et Al. (2009); Interpolation of the MESA results to the Basu points; Comparison between simulation and experiment.

Furthermore, note how the $\delta c_s/c_s$ plot is substantially different from the `gs98` case. One can even see a sort of discontinuity, corresponding to the base of the Sun's convective layer, at $r/R_\odot \approx 0.7$, which closely matches other theoretical/experimental predictions, like, e.g., Ref. [8]'s, where $1 - r/R_\odot = 0.287 \pm 0.003$.

2.3 Comparison of the two models

We are now fully equipped to compared the two models: `gs98` and `a09`. The easiest, and most obvious, way to do this is to plot both $\delta c_s/c_s$ graphs in the same window. This is done below.
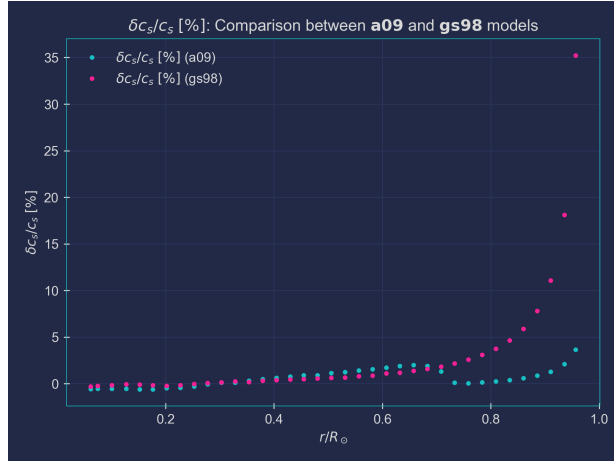
Figure 3: Comparison between simulation and experiment, for the two proposed models: Grevesse (1998) and Asplund (2009).

As can be seen, by this metric, the `a09` model appears to be ever so slightly better, since the relative error (relative to Basu's data) is, on average, smaller. Thus, from now on, we shall choose to use this model, instead of Grevesse's.

3 Part 2: Solar spectrum analysis

In this part of the work, we will look at the calibrated velocity time-series from the GOLF experiment, aboard SoHO, and compare its eigenfrequencies against those provided by the MESA simulations, through the GYRE package.

3.1 Simulation data: GYRE frequencies

As discussed previously, we will make use of GYRE, coupled with MESA, to obtain the desired eigenmode

frequencies. Note that the simulations consider the `a09` model, naturally following from Part 1's discussion. Additionally, we feed GYRE the following parameters:

1. `grid_type = 'LINEAR'`;
2. `freq_min = 5`;
3. `freq_max = 5000`;
4. `freq_min_units = 'UHZ'`;
5. `freq_max_units = 'UHZ'`;
6. `n_freq = 1000`.

As such, GYRE will compute 1000 eigenmodes, whose frequencies lie in the interval $[5, 5000]$ μHz[3].

3.2 Experimental data: GOLF experiment

The calculation of the eigenmode frequencies is significantly more involved in GOLF's case, since we only have access to the calibrated velocity time-series. Thus, in order to obtain the desired frequency data, we will need to *Fourier* transform said time-series. Before that, though, there is another problem we need to solve: The GOLF experiment encompasses two photomultipliers, which are each calibrated using two different methods: 1 - Paris and 2 - Los Angeles. Each combination of photomultiplier and calibration method is accompanied by a corresponding data-set. However, we need only use one of these data-sets. Thus, we are interested in figuring out which of these is the best. Said analysis is what follows. The first thing we do is plotting all four data-sets.
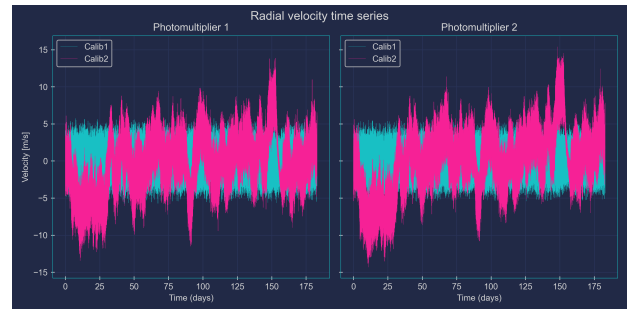

Figure 4: Radial velocity time series, from the GOLF experiment, for two of its photomultipliers, using two different calibration methods: 1 - Paris, 2 - Los Angeles.

As can be seen, the results vary drastically between calibration methods. Either way, we expect the Sun to have a relatively regular behaviour during the observation period (183 days in total), which is what is observed for calibration method 1. The large oscillations in calibration method 2 do not seem to

[3]In some of my plots, I might have altered this upper limit, so I could study the asymptotic limit of, e.g., the large and small separations.

come from the Sun. Rather, they most likely correspond to some anomaly in this calibration, which is why we shall discard these data-sets and focus on calibration method 1, instead. Additionally, as there does not seem to be much of a difference between the two photomultipliers, we opted to use photomultiplier 1. However, we could have also used an averaged signal, from the two photomultipliers, which would have been more thoughtful and, potentially, better.

Before plotting the *Fourier* spectrum, we decided to plot a spectrogram, for visualization purposes.
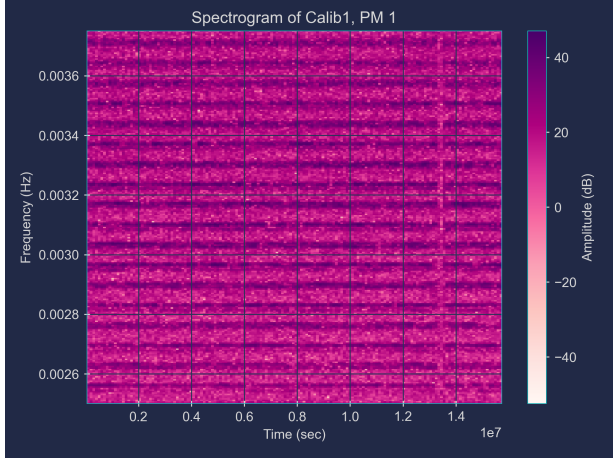
Figure 5: Radial velocity time series spectrogram. Used photomultiplier 1, with calibration method 1 (Paris). The many frequency modes of the Sun's radial oscillation are already visible here.

Here, one can already see the many eigenmode frequencies of the Sun, which correspond to the dark purple lines, in Figure 5. If we want to obtain more detailed information, though, we have to plot the actual *Fourier* spectrum. Together with the MESA/-GYRE frequencies, this is presented below, in Figure 7, separately, for each angular degree, l. If we were to, instead, plot everything in a single window, Figure 6 would be obtained.
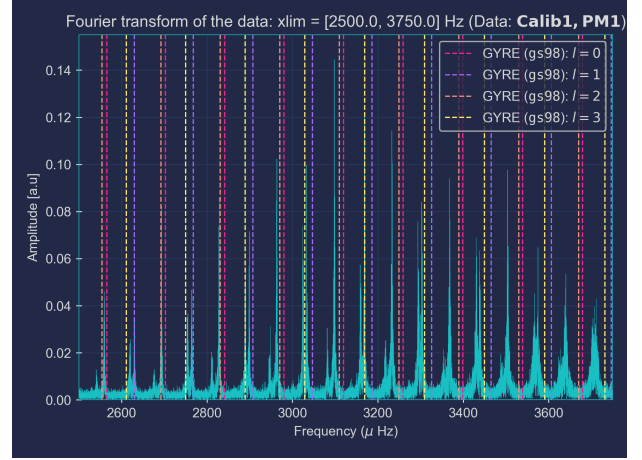

Figure 6: Fourier transform of the chosen time series: Photomultiplier 1, with calibration method 1. This is plotted alongside the frequency modes obtained from the MESA simulation, using the GYRE module. (Here, all in the same plot.)
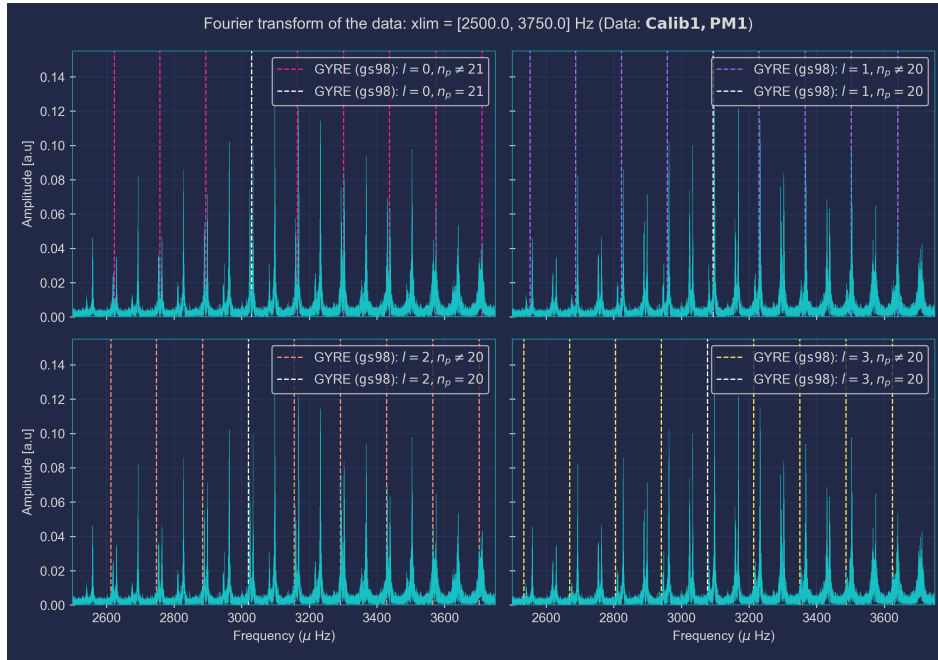

Figure 7: Fourier transform of the chosen time series: Photomultiplier 1, with calibration method 1. This is plotted alongside the frequency modes obtained from the MESA simulation, using the GYRE module.

From this [GOLF's] data, we intend to extract the frequencies of the peaks, through fitting against Lorentzian curves, and identify them with the correct eigenmode (quantum numbers: n and l), so that we can compare the results with what GYRE provides us. This fitting procedure, however, is rather complex and tedious. As such, we will first focus on the analysis of GYRE's eigenfrequency results.

3.3 Large and small separations: MESA/GYRE

As previously discussed, we are interested in determining the large and small separations of our data. This is shown below, for MESA/GYRE.
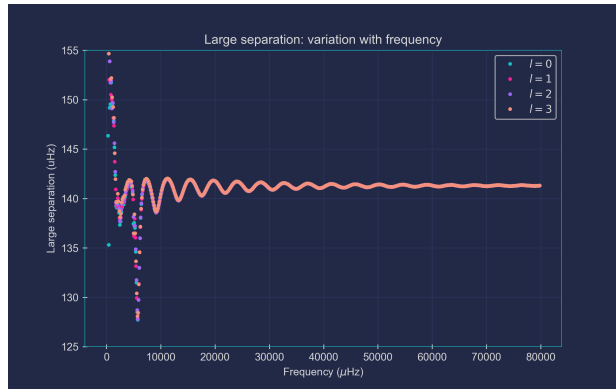
(a) Large separation (MESA/GYRE).
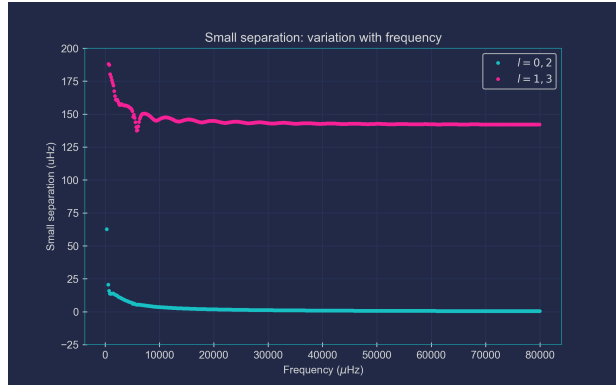
(b) Small separation (MESA/GYRE).

Figure 8: Large and small separations, computed using the obtained frequency modes from GYRE. One can clearly see how both of them tend to a specific asymptotic value, as predicted theoretically.

Here, the large separation was computed using Eq. (4), whereas the small separation was calculated using: $\delta\nu_{l,l+2} = \nu_{n+1,l} - \nu_{n,l+2}$ (All of this is built into the `Stellar_freqs` class, in FourierAnalysis.ipynb). The results match reasonably well with what is expected from previous experimental studies, namely,

from Refs. [9] and [10] (GOLF papers); all but the small separation for $l = 1, 3$! For some reason, that I have yet to figure out, the values for $\delta\nu_{1,3}$ are all unreasonably high, especially when compared to $\delta\nu_{0,2}$. In an attempt to correct this problem, we tried to compute the asymptotic small separation, through the rightmost part of Eq. (5). The obtained results are presented below.
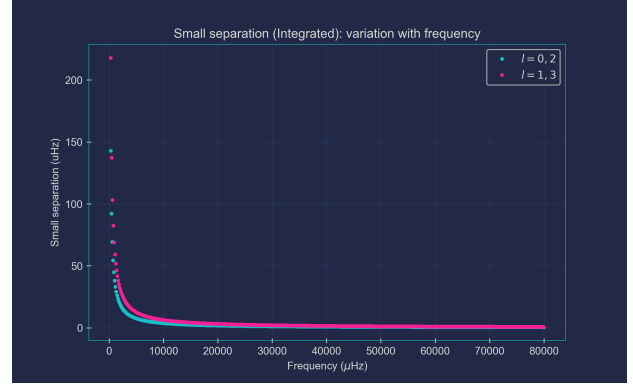

Figure 9: MESA/GYRE: Asymptotic small separation, computed using the rightmost part of Eq. (5).

This time, the values appear to match experimental observations much more adequately.

3.4 Large and small separations: GOLF & Comparisons

Now, we have to go back to the fitting problem. The best way to extract the eigenfrequencies from the *Fourier* spectrum is, exactly, to fit each of these peaks to a Lorentzian curve, according to:

$$L(x) = A \frac{\Gamma/2}{(x - x_0)^2 + (\Gamma/2)^2}, \qquad (7)$$

where A represents a scaling factor, Γ corresponds to the peak's Full Width at Half Maximum (FWHM, for short) and x_0 is its center. Since the peaks show up in pairs, we opted to fit them pairwise, as well. Our algorithm will sweep through the *Fourier* spectrum, in windows of size approximately equal to the large separation, fitting two peaks at a time. Before fitting, though, we employ a peak finding algorithm. However, doing this with the original signal is not too great of an idea, due to the high frequency oscillations (in the *Fourier* spectrum), similar to noise[4], that plague the data. To solve this problem, we apply a Savitzky-Golay filter (with `polynomial_order = 3, window_size = 90`), before utilising the peak finder algorithm (scipy's `find_peaks`). Then, for each window, if two peaks were successfully found[5], the algorithm proceeds with

---

[4]Stochastic noise, actually.

[5]This is so we have an easier time tagging them with their correct n and l quantum numbers.

the fitting, which is done using scipy's `curve_fit`. Additionally, a genetic algorithm is utilised to generate initial values for the Lorentzian parameters, so we have an overall easier time with the fitting (i.e., faster fitting). This includes, naturally, the utilisation of the previously found peak values as an initial estimate to x_0 [6]. All of this is built into the `Progressive_Lorentz_Fitter` class, in FourierAnalysis.ipynb. Examples of the fitting procedure, in action, are presented below. The fitting parameters are also shown.
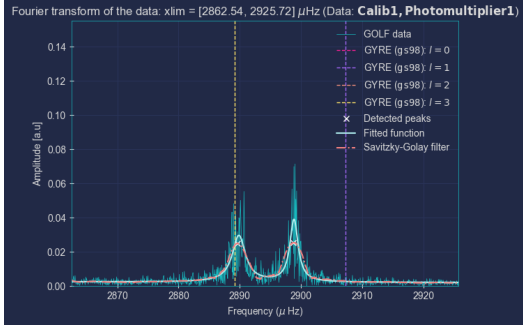
Figure 10: Fitting algorithm: application to the GOLF data, for `xlim = [2862.54, 2925.72] uHz`.

Fit parameter	1st Peak	2nd Peak
A [μHz · a.u.]	0.111 ± 0.006	0.093 ± 0.004
Γ [μHz]	2.611 ± 0.173	1.635 ± 0.099
x_0 [μHz]	2889.852 ± 0.057	2898.846 ± 0.034
a [a.u.]	(-7.057 ± 8.329) $\times 10^{-6}$	
b [μHz^{-1}]	(2.281 ± 2.411) $\times 10^{-2}$	

Table 1: Fit parameters, for the two peaks in the `xlim = [2862.54, 2925.72] uHz` window.

Remember that we fit the two Lorentzians at the same time, i.e., we are looking to minimize the sum of squared errors relative to an expression of the form: $f(x) = L_1(x) + L_2(x) + ax + b$, where $ax + b$ represents a small linear off-set, which helps with the fitting. Note that $L_n(x)$ is defined as in Eq. (7).
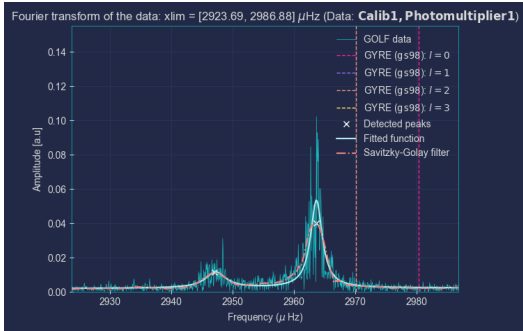

Figure 11: Fitting algorithm: application to the GOLF data, for `xlim = [2923.69, 2986.88] uHz`.

Fit parameter	1st Peak	2nd Peak
A [μHz · a.u.]	0.059 ± 0.009	0.186 ± 0.006
Γ [μHz]	4.065 ± 0.794	2.330 ± 0.104
x_0 [μHz]	2947.208 ± 0.247	2963.654 ± 0.034
a [a.u.]	(0.491 ± 1.043) $\times 10^{-5}$	
b [μHz^{-1}]	(-1.218 ± 3.085) $\times 10^{-2}$	

Table 2: Fit parameters, for the two peaks in the `xlim = [2923.69, 2986.88] uHz` window.

It took me quite some time to be able to develop this algorithm, since I wanted to make it automatic, for any data-set, of any given origin. Note, however, that the frequencies too far away from the central peak (≈ 3.1 mHZ) absolutely cannot be reliably fit, since they are very hard to detect in the data, due to the ever present stochastic noise. At the end of the day, though, I am fairly happy with the developed code. Note that due to my scarce background in astrophysics (I did not take the Astrophysics course, from Prof. Ilídio), I opted to focus harder on the data science aspect of this work, and I think it shows.

At this point, we are finally ready to plot the large and small separations for the GOLF data. These results are shown below, followed by the MESA/GYRE results, in the same frequency window, for easier comparison between the two.

(a) Large separation (GOLF).

(b) Small separation (GOLF).

Figure 12: Large and small separations, computed using the obtained frequency modes from the GOLF data (after double Lorentzian fitting).
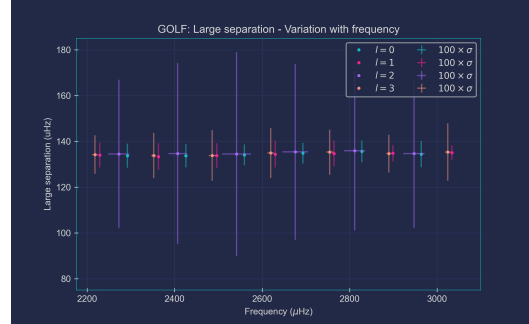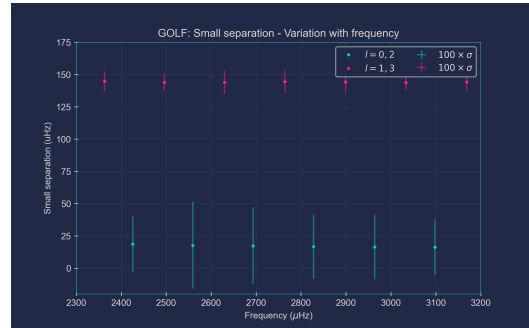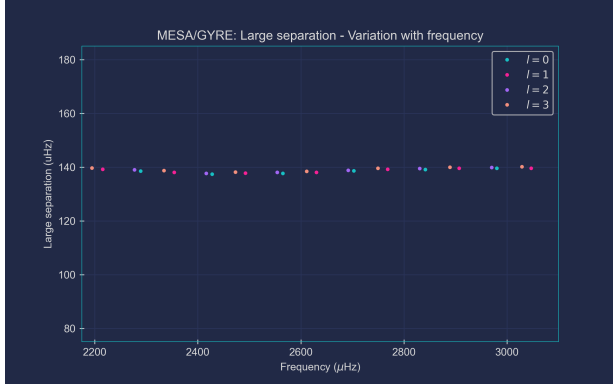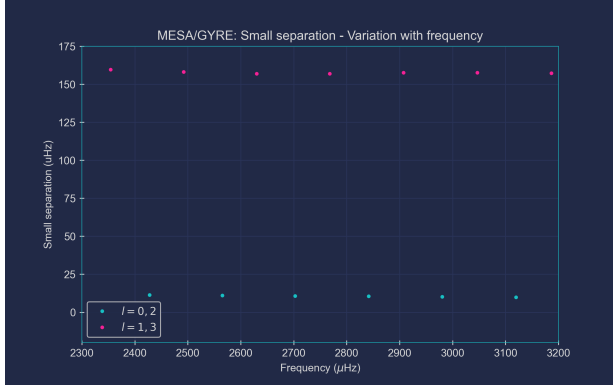
---

[6]We note that there's many more intricacies to the code that we do not explain here, due to page limitations. Either way, the complete developed code is provided in the following GitHub repository, which we have created for this project only: https://github.com/kaiuki2000/Helioseismology_Project/tree/main

(a) Large separation (MESA/GYRE) - detail.

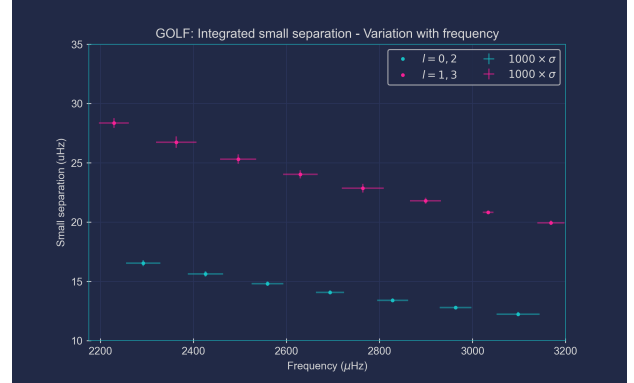(b) Small separation (MESA/GYRE) - detail.

Figure 13: Large and small separations, computed using the obtained frequency modes from GYRE. Now, we show the same frequency window as in the GOLF case, to facilitate the comparison. Note how the GYRE values do not come with an uncertainty. This appears to be a particularity of GYRE (which I could not, unfortunately, go around.)

Note how the error bars, in Figures 12a and 12b are multiplied by 100, which indicates very accurate values. Once again, the results match reasonably well with what is expected from previous works on the matter; except for the small separation case, when $l = 1, 3$, for which the same discrepancies as before [for MESA/GYRE] show up again in GOLF. Either way, the two models (MESA/GYRE and GOLF) appear to agree in their predictions, which is rather relieving.

Once again, in an attempt to correct the small separation values, for $l = 1, 3$, we made use of the asymptotic small separation limit, just like we did before. The obtained results are shown in Figures 14a and 14b, below.

Note how, again, the uncertainties are multiplied, this time by 1000. As can be seen, the small separation values do, now, agree better with what was expected. Unfortunately, I was not able to discover why the approximate formula, $\delta\nu_{l,l+2} = \nu_{n+1,l} - \nu_{n,l+2}$,

yielded such outlandish results (for $l = 1, 3$). The systematic error in both MESA/GYRE and GOLF appears to suggest that there is some mistake in how this small separation is computed. However, I checked some of these results manually and the values were, indeed, correct. This is, definitely, something that I would have liked to investigate further, had I had more time in my hands. For now, though, we will have to settle for these results.

(a) Asymptotic small separation (GOLF) - detail.
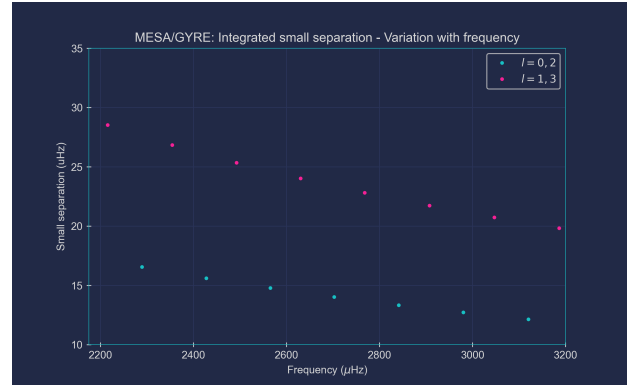
(b) Asymptotic small separation (MESA/GYRE) - detail.

Figure 14: Asymptotic small separations, computed using the rightmost part of Eq. (5). We show the same frequency window for both models, to facilitate the comparison.
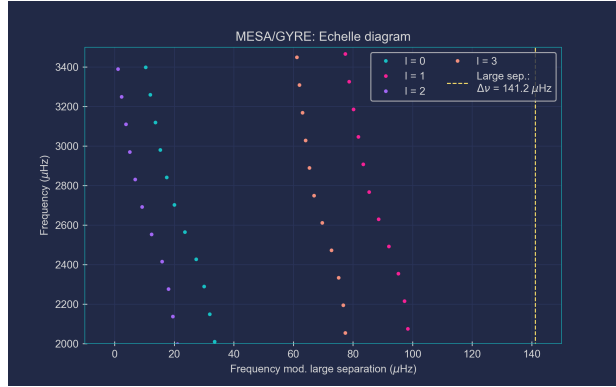
4 Echelle diagrams

In addition to the previous analysis, I also decided to plot the *Echelle* diagrams, for both MESA/GYRE and GOLF's values, which resulted in the following plots, below. Since the p-modes, for a certain l, are expected to be evenly spaced, separated by the large separation, $\Delta\nu$, we expect the *Echelle* diagram to be comprised of rough vertical ridges, for each angular degree, l. This can be seen in Figures 15a and 15b. Although not exactly 100% vertical, the lines somewhat match the expected output. We also note that the GOLF and MESA/GYRE results appear to be

off-set, by about 20 μHz. This is, most likely, due to the small differences in the large separation values between these two models, which propagate to the *Echelle* diagram, as one would expect.
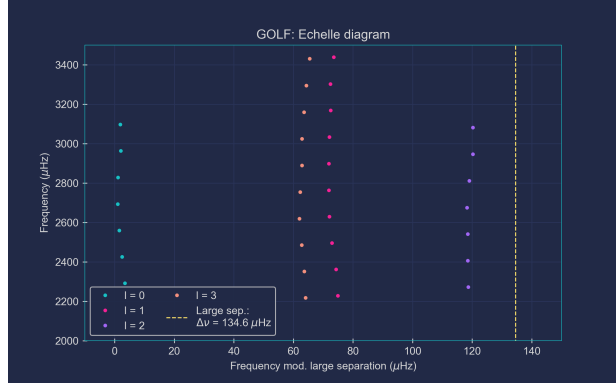
(a) Echelle diagram - GOLF.

(b) Echelle diagram - MESA/GYRE.

Figure 15: Echelle diagrams, obtained for both GOLF and MESA/GYRE's results.

5 Conclusion

Helioseismology has, without a doubt, revolutionized our understanding of the Sun's internal structure. The study of its radial oscillations is the primary means through which this is performed. In this work, we delved into some of the concepts behind the theory of these oscillations and how they can be used to probe the Sun's interior. Extra emphasis was put on the large and small separation analyses of the data, since they provide us with firsthand information on the Sun's internal composition (density, e.g.) and age, respectively. Very much like how we examined the Sun, all of these techniques could also be employed in the study of other, inherently different, stars, expanding Helioseismology into the more general field that is known as Asteroseismology. As a follow-up to this work, it would be interesting to extend this analysis to a different star, with the intent of evaluating how my developed workflow performs under various distinct conditions. Either way, we are reasonably happy with the obtained results, overall.

References

[1] S. Turck-Chièze, S. Basu, S. Brun, J. Christensen-Dalsgaard, A. eff darwich, I. Lopes, F. Hernández, G. Berthomieu, J. Provost, R. Ulrich, F. Baudin, P. Boumier, J. Charra, A. Gabriel, R. García, G. Grec, C. Renaud, J. Robillot, and T. Cortes, "First View of the Solar Core from Golf Acoustic Modes," *Solar Physics*, vol. 175, pp. 247–265, 01 1997. [Online]. Available: https://link.springer.com/article/10.1023/A:1004992727541

[2] H. Schunker, J. Schou, P. Gaulme, and L. Gizon, "Fragile Detection of Solar *g* modes by Fossat et *al.*" *Solar Physics*, vol. 293, no. 6, jun 2018. [Online]. Available: https://doi.org/10.1007%2Fs11207-018-1313-6

[3] M. Tassoul, "Asymptotic approximations for stellar nonradial pulsations." , vol. 43, pp. 469–490, Aug. 1980. [Online]. Available: https://ui.adsabs.harvard.edu/abs/1980ApJS...43..469T

[4] J. Christensen-Dalsgaard, "Helioseismology," *Reviews of Modern Physics*, vol. 74, no. 4, pp. 1073–1129, nov 2002. [Online]. Available: https://doi.org/10.1103%2Frevmodphys.74.1073

[5] N. Grevesse and A. J. Sauval, "Standard Solar Composition," vol. 85, pp. 161–174, May 1998, provided by the SAO/NASA Astrophysics Data System. [Online]. Available: https://ui.adsabs.harvard.edu/abs/1998SSRv...85..161G

[6] M. Asplund, N. Grevesse, A. J. Sauval, and P. Scott, "The Chemical Composition of the Sun," *Annual Review of Astronomy and Astrophysics*, vol. 47, no. 1, pp. 481–522, Sep 2009. [Online]. Available: https://doi.org/10.1146%2Fannurev.astro.46.060407.145222

[7] S. Basu, W. J. Chaplin, Y. Elsworth, R. New, and A. M. Serenelli, "Fresh insights on the structure of the solar core," *The Astrophysical Journal*, vol. 699, no. 2, pp. 1403–1417, jun 2009. [Online]. Available: https://doi.org/10.1088%2F0004-637x%2F699%2F2%2F1403

[8] J. Christensen-Dalsgaard, D. O. Gough, and M. J. Thompson, "The Depth of the Solar Convection Zone," vol. 378, p. 413, Sep 1991, provided by the SAO/NASA Astrophysics Data System. [Online]. Available: https://ui.adsabs.harvard.edu/abs/1991ApJ...378..413C

[9] S. Turck-Chièze, S. Basu, S. Brun, J. Christensen-Dalsgaard, A. eff darwich, I. Lopes, F. Hernández, G. Berthomieu, J. Provost, R. Ulrich, F. Baudin, P. Boumier, J. Charra, A. Gabriel, R. García, G. Grec, C. Renaud, J. Robillot, and T. Cortes, "First view of the solar core from golf acoustic modes," *Solar Physics*, vol. 175, pp. 247–265, 01 1997.

[10] M. Lazrek, F. Baudin, L. Bertello, P. Boumier, J. Charra, D. Fierry-Fraillon, E. Fossat, A. H. Gabriel, R. A. García, B. Gelly, C. Gouiffes, G. Grec, P. L. Pallé, F. Pérez Hernández, C. Régulo, C. Renaud, J. M. Robillot, T. Roca Cortés, S. Turck-Chièze, and R. K. Ulrich, "First Results on it P Modes from GOLF Experiment," , vol. 175, no. 2, pp. 227–246, Oct. 1997.

[11] "MESA GitHub repository," https://github.com/MESAHub/mesa, Accessed: 2023-11-05.

[12] "GYRE GitHub repository," https://github.com/rhdtownsend/gyre, Accessed: 2023-11-05.